Formation of periodic surface structures in multilayer amorphous $Ge_2Sb_2Te_5$ thin films irradiated by femtosecond laser pulses

View the article online for updates and enhancements.

Formation of periodic surface structures in multilayer amorphous Ge₂Sb₂Te₅ thin films irradiated by femtosecond laser pulses

A V Kolchin[1], D V Shuleiko[1,2], S V Zabotnov[1,2], L A Golovan[1,2], D E Presnov[1,3,4],

T P Kaminskaya[1], P I Lazarenko[5], S A Kozyukhin[6,7], P K Kashkarov[1]

[1]Lomonosov Moscow State University, Faculty of Physics, 119991, Moscow, Leninskie Gory 1/2, Russia
[2]Big Data Storage and Analysis Center of Lomonosov Moscow State University, 119192, Moscow, Lomonosovsky Avenue 27/1, Russia
[3]Skobeltsyn Institute of Nuclear Physics of Lomonosov Moscow State University, 119991, Leninskie Gory 1/2, Moscow, Russia
[4]Quantum Technologies Center of Lomonosov Moscow State University, 119991, Leninskie Gory 1/35, Moscow, Russia
[5]National Research University of Electronic Technologies «MIET», 124498, Zelenograd, Shokina Square 1, Russia
[6]N S Kurnakov Institute of General and Inorganic Chemistry of RAS, 119991, Moscow, Leninskiy Avenue 31, Russia
[7]National Research Tomsk State University, 634050, Tomsk, Lenina Avenue 36, Russia

avkolchin@physics.msu.ru

Abstract. Phase transitions and periodic surface modification in amorphous Ge₂Sb₂Te₅ thin films on multilayer substrate were revealed as a result of the samples irradiation by femtosecond laser pulses with the wavelength of 1250 nm. Raman spectroscopy revealed partial crystallization in the treated samples. Calculations and analysis of scanning electron and atomic-force microscopy data showed that formation of the periodic surface structures is related to photoinduced surface plasmon-polariton excitation and depends on laser radiation fluence. The obtained results are useful for design and fabrication of new promising data-storage and polarization optics devices.

1. Introduction

Telluride-based chalcogenide materials such as Ge₂Sb₂Te₅ (GST225) are widely used as a basic material for rewritable and non-volatile memory technologies [1], reconfigurable nanophotonic devices for post-von Neumann arithmetic processing [2], as well as metasurfaces [3]. In the case of optical data storage techniques, data recording is achieved by laser-induced direct and reverse phase transitions between amorphous and crystalline states in the irradiated material [4]. Readout is based on difference between optical properties of the amorphous and crystalline phases [5]. Use of femtosecond

laser pulses allows increasing the speed and energy efficiency for the phase transitions due to non-thermal character of induced crystallization or amorphization processes [6].

Additionally, femtosecond laser irradiation leads to formation of laser-induced periodic surface structures (LIPSS or «ripples») on metals, semiconductors and dielectrics [7]. Formation of the ripples is explained by interference between an incident laser beam and excited surface electromagnetic waves (SEWs) – plasmon-polaritons [8]. The period of such surface structures depends on a wavelength of incident laser radiation and photo-induced free charge carriers concentration [9]. In turn, the LIPSS possess artificial anisotropy [10] that can be promoted in fabrication of new polarization optical devices and optical data recording [11].

Earlier, LIPPS fabrication in GST225 films was performed using laser radiation with the wavelength of 351 nm [12] or 515 nm [13] where absorbance is strong. Treatment by near-infrared femtosecond laser pulses is also of great interest, as relatively small absorption and reflection coefficients in this spectral region facilitate more effective penetration of the radiation into the material. Therefore, in this work we form LIPSS in amorphous GST225 thin films on metallic multilayer substrates using femtosecond laser irradiation with the wavelength of 1250 nm.

2. Materials and methods

Amorphous GST225 films with 100 nm thickness were deposited by direct current (DC) magnetron sputtering at room temperature on a W(140 nm)/TiN(30 nm)/SiO$_2$(1 μm)/Si(substrate) multilayer structure. The residual pressure in the chamber before the deposition was $3 \cdot 10^{-3}$ Pa, and the pressure of Ar during the process was $5.7 \cdot 10^{-1}$ Pa. The sputtering power was 100 W. The uniformities of the element distributions across the thicknesses and structure of the fabricated films were controlled by Auger electron spectrometry and X-ray diffraction analysis.

A spectroscopic ellipsometer was used to measure the optical constants in the 190 – 2100 nm range with wavelength steps of 5 nm. To extract the refractive index and extinction coefficient for amorphous GST225 thin film, the ellipsometric spectra were evaluated by a PsiDelta program using five-layered model (air-surface-GST225-SiO$_2$-Si).

The samples were irradiated by femtosecond laser pulses (λ=1250 nm, ν=10 Hz, τ=125 fs) with linear polarization at normal incidence. The energy fluence J in each laser pulse was 0.14 J/cm^2 or 1.17 J/cm^2. The pulse number was 70 or 20, respectively.

Images of treated surface were obtained by an NT-MDT SolverPro atomic force microscope (AFM) and a Carl Zeiss Supra 40 scanning electron microscope (SEM). Phase changes were observed via Raman microscope Horiba Jobin Yvon HR800 using Ar$^+$ laser excitation (488 nm, 10 mW).

The formation of LIPSS is caused by modulated surface ablation due to interference of the SEW and incident laser radiation [8, 9]. SEW excitation conditions between two media with the dielectric constants ε_1 and ε_2 at a frequency ω are:

$$\Re(\varepsilon_2(\omega)) < 0, |\Re(\varepsilon_2(\omega))| > \Re(\varepsilon_1(\omega)) > 0. \tag{1}$$

Here ε_1=1 corresponds to air, ε_2 is the dielectric constant of amorphous GST225 thin film during the irradiation.

The real part of the dielectric constant Re(ε) is described by Drude Model [8, 9]:

$$\Re(\varepsilon(\omega)) = \varepsilon_\infty - \frac{\omega_p^2}{\omega^2 + \gamma^2}, \tag{2}$$

$$\omega_p^2 = \frac{4\pi N e_0^2}{m}, \tag{3}$$

where ω_p is the plasmonic frequency, N is the non-equilibrium charge carriers concentration, γ is the collision frequency, ε_∞ is the static dielectric constant, m^* and e_0 are the electron effective mass and charge respectively.

The conditions (1) mentioned above can be realized if the concentration of free charge carriers reaches threshold value:

$$N_0 = \frac{(\omega^2 + \gamma^2)\varepsilon_\infty m}{4\pi e_0^2}. \tag{4}$$

High concentration N of non-equilibrium charge carriers in amorphous GST225 thin films can be achieved under high-power femtosecond laser pulsed treatment. In this case generation of the electrons is described by the following differential equation:

$$\frac{dN}{dt} \approx \frac{\alpha(1-R)I(t)}{\hbar\omega},$$ (5)

where α and R are the absorption and reflection coefficients, respectively, $I(t)$ is the time-dependent laser radiation intensity.

The period of surface ripples formed at normal incidence and oriented orthogonally to the laser radiation polarization is estimated by the formula [9]:

$$\Lambda = \lambda\sqrt{\frac{1+\Re(\varepsilon_2)}{\Re(\varepsilon_2)}}.$$ (6)

3. Experimental results

The refractive index and extinction coefficient measured by ellipsometry and presented in fig. 1a. Subsequent calculations show that observed initial amorphous GST225 thin films demonstrate low absorption and reflection in near-infrared optical range (fig. 1b). The absorption and reflection coefficient values are α=24500 cm^{-1} and R=0.39, respectively, for the λ=1250 nm. These values seem to be favorable for penetration and propagation of the laser pulses used for LIPSS fabrication.
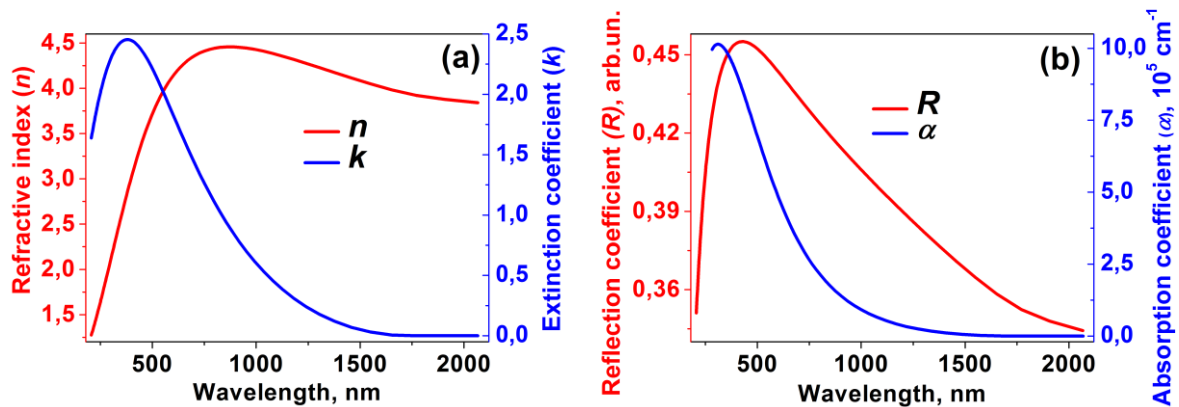
Figure 1. Measured spectra of the refractive index and extinction coefficient of initial amorphous GST225 films (a), corresponding calculated reflection and absorption coefficients (b).

Raman spectra for the GST225 films before and after irradiation are presented in fig. 2. The wide band in the range of 110 – 170 cm^{-1} corresponds to GST225 alloy [14].
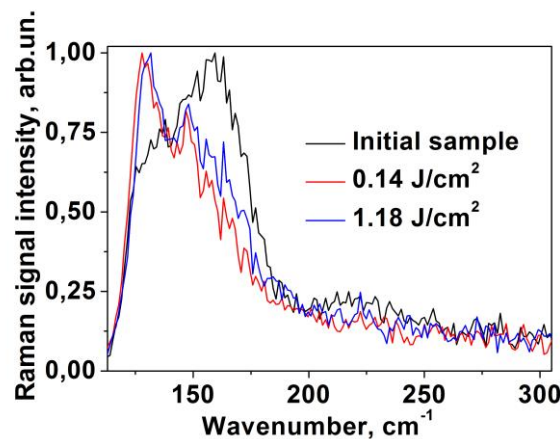
Figure 2. Raman spectra of the initial amorphous GST225 thin film and the films irradiated by femtosecond laser pulses with different fluence.

Change of ratio between $GeTe_4$ (110-140 cm^{-1}) and Sb_2Te_3 (140-170 cm^{-1}) peaks as a result of femtosecond laser irradiation is explained as partial crystallization of amorphous regions.

SEM images (fig. 3a,c) show the formation of the LIPSS, which are perpendicular to the polarization vector of the modifying laser radiation. After irradiation at the fluence 0.14 J/cm^2 the surface structures constitute regular one-dimensional lattice with the period Λ_1=1.17±0.02 µm and the depth H_1=10 – 20 nm (fig. 3a,b). In turn, the laser pulses with the higher fluence 1.17 J/cm^2 induce formation of discontinuous ripples with period Λ_2=0.91±0.02 µm and the depth H_2=100 – 200 nm (fig. 3c,d).
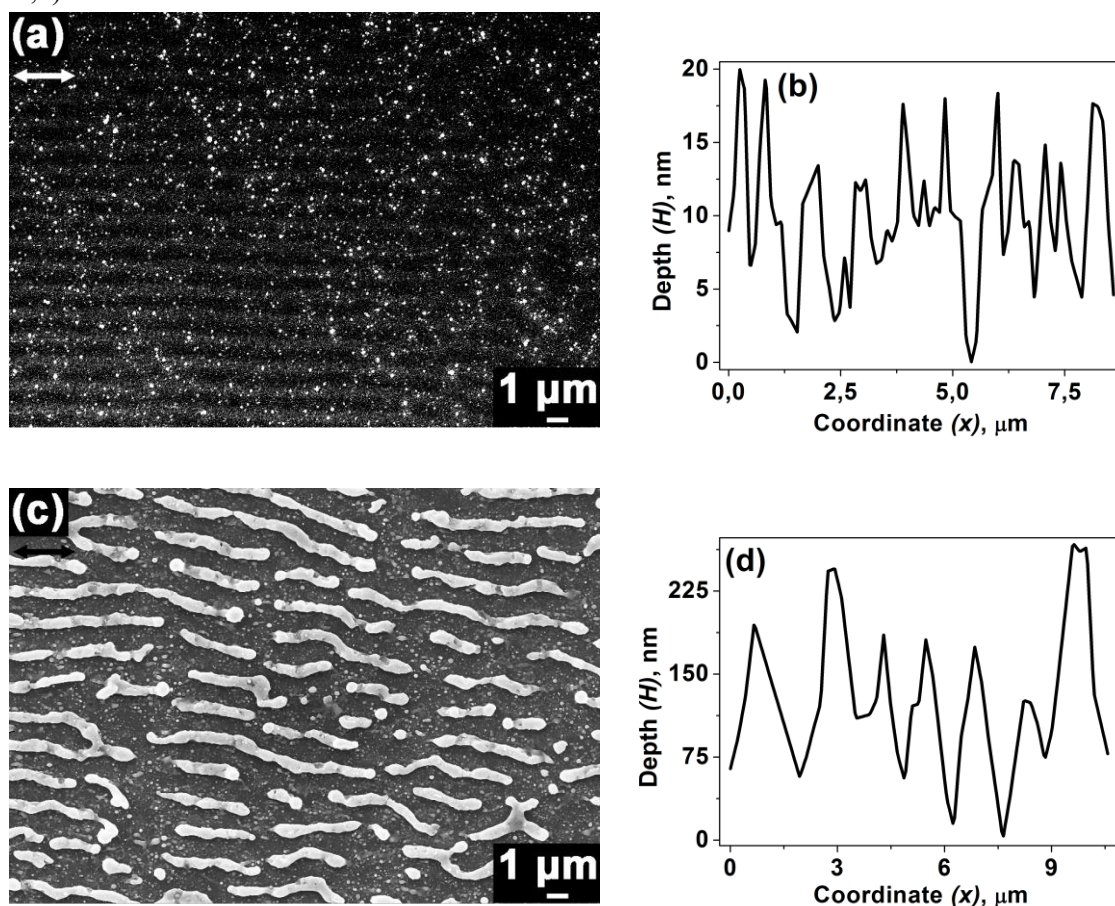
Figure 3. SEM images and AFM profiles of regions irradiated by femtosecond laser pulses with fluences 0.14 J/cm^2 (a, b) and 1.17 J/cm^2 (c, d).

Formation of the observed LIPSS (fig. 3) in the amorphous GST225 thin films is possible when the SEW excitation conditions (1) are satisfied. These conditions are realized when the non-equilibrium charge carriers concentration exceeds the threshold value of N_0=1.7·10^{21} cm^{-3} which is determined from (4) and data from [15]. According to equation (5) and data presented in fig. 1b femtosecond laser irradiation at the fluences from 0.14 to 1.17 J/cm^2 allows to induce non-equilibrium carriers with the concentration $N(\tau = 125$ fs$) \approx (0.5 - 4.5) \cdot 10^{22}$ cm^{-3} at a single pulse action, which is larger than the threshold value N_0. For multiple irradiation by 20 or 70 laser pulses in the conditions of our experiments the non-equilibrium carriers concentrations N_1=6·10^{21} cm^{-3} and N_2=2.8·10^{21} cm^{-3} were estimated by formula (2), (3) and (6) for the obtained ripples with the periods Λ_1 and Λ_2, respectively. These values are larger N_0 and the condition (1) is hold true too. Therefore, the performed estimations indicate that the formation of orthogonal to laser beam polarization LIPSS in amorphous GST225 thin

films is caused by the interference of femtosecond pulsed laser radiation and photoinduced in the near-surface layer plasmon-polaritons. The role of metallic wolfram sublayer is not obvious at that.

4. Conclusion

Femtosecond laser-induced phase modification in bulk and periodic structure formation at the surface of amorphous GST225 thin films deposited on multilayer substrates was realized by the radiation of near infrared region. Raman spectroscopy data demonstrate presence of GST225 alloy in the irradiated samples. Partial crystallization of amorphous regions was observed as a result of femtosecond laser treatment.

The obtained LIPSS period is comparable with the wavelength of modifying radiation. Fabrication of such structures is caused by interference of incident laser beam with excited plasmon-polaritons and consequent periodically modulated ablation of the surface. Calculations confirm this hypothesis.

The obtained results enhance understanding of the surface modification and phase transition mechanisms in amorphous GST225 thin films under femtosecond pulsed laser treatment, as well as give new knowledge on experimental conditions required for LIPSS formation for fabrication of new promising data-storage and polarization optics devices.

References

[1]   Guo P, Sarangan A M, Agha I 2019 *Appl. Sci.* **9(3)** 530
[2]   Feldmann J, Youngblood N, Wright C D, Bhaskaran H, Pernice W H P 2019 *Nature* **569** 208
[3]   Guo Z, Yang X, Shen F, Zhou Q, Gao J, Guo K 2018 *Sci. Rep.* **8** 12433
[4]   Han Z N, Han W N, Liu F R, Han Z, Yuan Y P, Cheng Z C 2020 *Nanotechnology* **31** 115706
[5]   Xu Z, Chen C, Wang Z, Wu K, Chong H, Ye H 2018 *RSC Adv.* **8** 21040
[6]   Ionin A A, Kudryashov S I, Samokhin A A 2017 *Phys. Usp.* **60** 149
[7]   Bonse J, Krüger J, Höhm S, Rosenfeld A 2012 *J. Laser Appl.* **24(4)** 042006
[8]   Martsinovsky G A, Shandybina G D, Dement'eva Y S, Dyukin R V, Zabotnov S V, Golovan' L A, Kashkarov P K 2009 *Semiconductors* **43** 1298
[9]   Martsinovskii G A, Shandybina G D, Smirnov D S, Zabotnov S V, Golovan' L A, Timoshenko V Yu, Kashkarov P K 2008 *Opt. Spectrosc.* **105** 67
[10]   Shuleiko D V, Potemkin F V, Romanov I A, Parhomenko I N, Pavlikov A V, Presnov D E, Zabotnov S V, Kazanskii A G, Kashkarov P K 2018 *Laser Phys. Lett.* **15** 056001
[11]   Zhang J, Drevinskas R, Beresna M, Kazansky P G 2015 *Appl. Phys. Lett.* **107** 041114
[12]   Yakovlev S A, Ankudinov A V, Vorobyov Yu V, Voronov M M, Kozyukhin S A, Melekh B T, Pevtsov A B 2018 *Semiconductors* **52** 809
[13]   Kozyukhin S, Lazarenko P, Vorobyov Yu, Baranchikov A, Glukhenkaya V, Smayev M, Sherchenkov A, Sybina Yu, Polohin A, Sigaev V 2019 *Opt. Laser Technol.* **113** 87
[14]   Wei T, Wei J, Zhang K, Zhao H, Zhang L 2017 *Sci. Rep.* **7** 42712
[15]   Shelimova L E, Karpinskii O G, Konstantinov P P, Kretova M A, Avilov E S, Zemskov V S 2000 *Inorganic Materials* **37(4)** 342